DMD 7856

# BIOTRANSFORMATION OF CARBON-14 LABELED MURAGLITAZAR IN MALE MICE: INTERSPECIES DIFFERENCE IN METABOLIC PATHWAYS LEADING TO UNIQUE METABOLITES

WENYING LI, DONGLU ZHANG, LIFEI WANG, HAO ZHANG, PETER T CHENG, DUXI ZHANG, DONALD W EVERETT, AND W GRIFFITH HUMPHREYS

Pharmaceutical Candidate Optimization (WL, DLZ, LW, DZ, DE, WGH), Discovery Chemistry (HZ, PTC), Pharmaceutical Research Institute, Bristol-Myers Squibb, Princeton, NJ 08543

1

DMD 7856

Running title: Biotransformation of muraglitazar in mice

Address correspondence to:

Donglu Zhang, Ph.D.

Pharmaceutical Candidate Optimization

Bristol-Myers Squibb Co.

P.O. Box 4000

Phone: 609-252-5582

Email: Donglu.Zhang@BMS.com

[1]Abbreviations used: ADME, absorption, distribution, metabolism, and excretion; BDC, bile duct cannulation; HPLC, high performance liquid chromatography; LC/MS, liquid chromatography/mass spectrometry; NMR: nuclear magnetic resonance; PPAR, peroxisome proliferator-activated receptor; TFA, trifluoroacetic acid.

# of text pages: 27

# of tables: 5

# of figures: 13

# of references: 13

# of word in abstract: 248

# of words in introduction: 270

# of words in discussion: 1316

DMD 7856

## ABSTRACT

Muraglitazar (Pargluva™), a dual alpha/gamma PPAR (peroxisome proliferator-activated receptor) activator, is under development for treatment of type 2 diabetes. This study describes the biotransformation profile of carbon-14 labeled muraglitazar in plasma, urine, feces, and bile samples from male CD-1 mice (intact and BDC) following single oral doses of 1 and 40 mg/kg. The major drug-related component circulating in mouse plasma was the parent compound for up to 4 h post dose. Similar to excretion profiles of muraglitazar in humans, monkeys, and rats, urinary excretion was minor and fecal excretion via the biliary route was the major elimination pathway for muraglitazar in mice. The parent compound was a minor component in urine, bile and feces, indicating that muraglitazar was extensively metabolized in mice. Major biotransformation pathways of muraglitazar in mice included taurine conjugate formation, acyl glucuronidation, hydroxylation, and *O*-dealkylation. In addition to those metabolites previously identified in humans, monkeys, and rats (M1-M21), several unique metabolites identified in mice included taurine conjugates (M24, M25, M26a,b,c and M31), oxazole-ring opened metabolites (M27 and M28), glutathione conjugates (M29a,b and M30), a dihydroxylated metabolite (M32), hydroxylated metabolites (M33 and M35), and a dehydrogenated metabolite (M34). The taurine conjugate of muraglitazar, M24, was a major metabolite in mice, accounting for 12-15% of the total dose in BDC mice or 7-12% of the total dose in intact mice. None of these taurine and glutathione conjugates were found in the bile samples of humans, monkeys, or rats.

3

DMD 7856

## INTRODUCTION

Muraglitazar (Pargluva[TM], BMS-298585, *N*-[(4-methoxyphenoxy)carbonyl]-*N*-[[4-2-(5-methyl-2-phenyl-4-oxazolyl)ethoxy] phenyl]methyl]glycine), a dual alpha/gamma PPAR (peroxisome proliferator-activated receptor) activator, is being developed to treat type 2 diabetes (Devasthale *et al.*, 2005). Muraglitazar was extensively metabolized in humans (Wang et al., 2005; Zhang et al., 2005). From a human ADME study, with the urine and feces collection, following a single 10 mg oral dose of [14C]muraglitazar, fecal excretion represented >90% of muraglitazar elimination and only oxidative metabolites were identified in feces of human subjects (Zhang et al., 2005). However, in a disposition study of [14C]muraglitazar in humans with bile collection following a single 20 mg oral dose, biliary excretion represented the major elimination pathway for muraglitazar and glucuronide conjugates were the major metabolites in the human bile (Wang et al., 2005). Seventeen oxidative metabolites and several glucuronide conjugates of [14C]muraglitazar have been identified in humans and presented previously (Zhang et al., 2005; Wang et al., 2005). These oxidative metabolites included hydroxy muraglitazar (M8a, M10, M11, and M14), *O*-demethyl muraglitazar (M15), *O*-demethyl hydroxy muraglitazar (M2, M5, M6, and M7), oxazole-ring opened metabolites (M9 and M16), *O*-dealkyl muraglitazar (M1), O-dealkyl *O*-demethyl muraglitazar (M21), dihydroxy muraglitazar (M3, M4, and M8), and muraglitazar 12-carboxylic acid (M12). For identification of oxidative metabolites, NMR data for M9, M10, M11, M14, and M16 were used and M5, M10, M11, and M12 were synthesized (Zhang et al., 2005). Glucuronide

4

metabolites included muraglitazar gluucronide (M13), the glucuronide of *O*-demethyl muraglitazar (M20), glucuronides of hydroxy muraglitazar (M18, 3 isomers), and glucuronides of hydroxy *O*-demethyl muraglitazar (M17, 3 isomers). Glucuronide metabolites were the major metabolites in human bile, however, the aglycones were found in feces, indicating hydrolysis in the intestines prior to excretion. Urinary elimination was very minor in humans (<5% of dose). Muraglitazar was the major circulating drug-related component in humans. Following oral administration of [$^{14}$C]muraglitazar to monkeys and rats, biliary elimination was also the major clearance pathway (data not shown).

In order to properly put into context any finding during toxicology or carcinogenicity studies, a thorough understanding of the biotransformation in the toxicology species relative to humans is necessary. This manuscript describes the metabolism of muraglitazar and characterization of unique metabolites including taurine and glutathione conjugates of [$^{14}$C]muraglitazar in male CD-1 (BDC and intact) mice.

## MATERIALS AND METHODS

**Materials.** [$^{14}$C]Muraglitazar (BMS-298585, *N*-[(4-methoxyphenoxy)carbonyl]-*N*-[[4-[2-(5-methyl-2-phenyl-4-oxazolyl)ethoxy] phenyl]methyl]glycine), 11.2 µCi/mg, 98.6% radiochemical purity) was synthesized at Bristol-Myers Squibb. The chemical structure and the position of the $^{14}$C-label are shown in Figure 1. Trifluoroacetic acid (TFA) and PEG-400 were purchased from Aldrich Chemical Co. (Milwaukee, WI). Ecolite$^{TM}$ liquid scintillation cocktail was purchased from ICN Biomedicals, Inc. (Costa Mesa, CA). Soluene-350 was purchased from PerkinElmer Life and Analytical Sciences (Boston, MA). All other organic solvents and the reagents were of HPLC grade or reagent grade. HPLC solvent A was 0.06% (v/v) TFA in water and HPLC solvent B was 0.06% (v/v) TFA in acetonitrile.

The bile samples from rats, monkeys, and humans were used in this study as comparators to mouse bile samples and they were collected for 0-24 h from rats (20 mg/kg dose), 0-48 h from monkeys (2 mg/kg dose), and 3-8 h from humans (10 mg/subject dose) after single oral administration of [$^{14}$C]muraglitazar as described previously (wang et al., 2005; Zhang et al., personal communication).

**Animal Studies**. The animal studies conformed to accepted criteria for care and use of laboratory animals, and complied with all applicable sections of the Final Rules of the Animal Welfare Act regulation (United States Department of Agriculture, Animal Welfare Act, 9 CFR 3, 1991).

The BDC mice were prepared at least 24 hour before dosing. Two 12-inch extension tubes (0.02" ID) were pulled through a spring tether with the use of a

wire hook and filled with 2.5% taurocholic acid solution prepared in 0.9% sterile saline. One tube was marked at both ends and used for bile duct connection. The other tube was used for duodenal end connection, one end of which was clamped off with a hemostat. The unanesthetized mouse was gently restrained while the cannula was externalized. The loop was cut and the tether end of the bile extension tube was expanded by dipping in xylenes for a few seconds. The bile end of the cannula was inserted into the expanded bile extension tube and the attachment sealed with a cyanoacrylate glue. The duodenum end of the cannula was inserted into the end of the other extension tube that had been expanded in xylenes and the attachment sealed with a cyanoacrylate glue. The hemostat attached to the bile extension tube was removed and the flow of bile into the extension tube was observed. The extension tubes were pulled through the tether until it rested close to the animal's body. The jacket was put on over the tether and secured with light orthodontic elastics. The extension tubes were then attached to a dual-channel swivel suspended beside the cage. The bile collection tube (0.012" ID) attached to the swivel was filled with 2.5% taurocholic acid. A solution of 2.5% taurocholic acid was infused through the swivel and into the duodenum at a rate of 0.4 mL/hour as a replacement fluid. The bile samples were collected by gravity flow.

As shown in Table 1, forty two CD-1 male mice were divided into four groups: group 1M (16 mice, intact) and group 3M (5 mice, bile-duct cannulated) received a single dose of 1 mg/kg; group 2M (16 mice, intact) and group 4M (5 mice, bile-duct cannulated) received a single dose of 40 mg/kg by oral gavage. The animals

were fasted for approximately 4 hour before dose administration. The dosing solutions of [$^{14}$C]muraglitazar were prepared in PEG-400 one day prior to the experiment and kept at room temperature. The actual amount of dosing solution administered to each animal was determined by weighing the loaded dosing syringe before dose administration and the emptied syringe after dose administration. The average doses for each groups were as following: 1M, $0.97 \pm 0.03$ mg/kg ($10.9 \pm 0.4$ $\mu$Ci/kg); 2M, $40.4 \pm 2.1$ mg/kg ($453 \pm 24$ $\mu$Ci/kg); 3M, $1.00 \pm 0.03$ mg/kg ($11.2 \pm 0.3$ $\mu$Ci/kg); and 4M, $40.6 \pm 1.0$ mg/kg ($455 \pm 11$ $\mu$Ci/kg). Four mice at each time point from group 1M and 2M were euthanized by asphyxiation with air/carbon dioxide gas followed by exsaguination *via* the abdominal vein at 1, 4, 12, or 24 h after dosing, and five mice in 3M and 4M group were euthanized at 24 h after dosing. Blood was collected in tubes containing K$_3$EDTA as the anticoagulant. After centrifugation, plasma was transferred into a labeled container and glacial acetic acid was added immediately (20 $\mu$L/mL of plasma). Bile was collected on dry ice for 0-24 h after dosing from group 3M and 4M. Glacial acetic acid was added to the bile samples (20 $\mu$L/mL bile) immediately upon thawing. Urine was collected on dry ice. A pooled 0-24 h urine sample was collected from four mice in the intact groups and 5 mice in the BDC groups. Glacial acetic acid was added to the urine samples (20 $\mu$L/mL urine) immediately upon thawing. Fecal samples were collected on dry ice. A pooled 0-24 h feces sample was collected from four mice in the intact groups and five mice from the BDC groups. Upon collection, fecal samples were weighed, ethanol/water (50:50, v/v) containing 2% glacial acetic acid (4 mL to 1 g

feces) was added, and then the samples were homogenized by a probe-type homogenizer. Unless otherwise noted, the pooled samples were obtained by combining half of each sample within the groups. All samples were stored at -20$^{\circ}$C.

**Preparation of Samples for Metabolite Profiling**.

**Bile.** A portion (0.5 mL) of the pooled bile sample (0-24 h) from group 3M and 4M was mixed with 0.5 mL of methanol, then centrifuged for 10 min at 2000x$g$. The supernatant was analyzed directly.

**Plasma.** Pooled plasma samples (1, 4, 12, and 24 h) were prepared by mixing 0.4 mL of plasma sample from each animal at each time point (groups 1M or 2M). One volume of pooled plasma sample was extracted twice with methanol/acetonitrile (50/50, v/v, four volumes each time). After the first addition of organic solvent, the sample was centrifuged at 2000x$g$ for 15 min. The supernatant was removed and the second portion of organic solvent was added to the pellet. The sample was vortexed to re-suspend the solid material, and centrifuged at 2000x$g$ for 15 min. The combined supernatants were evaporated to dryness under a stream of nitrogen. The samples were reconstituted in 500 $\mu$L of acetonitrile/HPLC solvent A (20/80, v/v) and centrifuged at 2000x$g$ for 15 min before HPLC injection. The radioactivity recovery from the plasma extraction procedure was 95, 94, 72, and 61% for the 1, 4, 12, and 24 h samples, respectively, from group 1M (1 mg/kg dose), and 95, 89, 73, and 59% for the 1, 4, 12, and 24 h samples, respectively, from group 2M (40 mg/kg dose). The low

DMD 7856

overall level of radioactivity from the 24 h plasma might have contributed to the low extraction recovery at the late time points.

**Urine.** Prior to HPLC analysis, the pooled urine sample (0-24 h) from each group was centrifuged for 10 min at 2000x*g* to remove any insoluble material.

**Feces.** The pooled feces homogenate sample (2 mL) was extracted twice with methanol/acetonitrile (50/50, v/v, 8 mL each time). After the first addition of organic solvent, the sample was centrifuged at 2000x*g* for 15 min. The supernatant was removed and a second portion of organic solvent was added to the pellet. The sample was vortexed to re-suspend the solid material and centrifuged at 2000x*g* for 15 min. The combined supernatants were evaporated to dryness at room temperature under a stream of nitrogen. The sample was reconstituted with 1 mL of HPLC solvent A/solvent B (80:20, v/v) and centrifuged before HPLC injection.

**Determination of Radioactivity Recovery.** Aliquots of the bile, plasma, or urine (25-100 μl) was mixed with Ecolite™ liquid scintillation cocktail (about 5 mL) and the amount of radioactivity was measured in a Packard Tri-Carb 2250 liquid scintillation counter (PerkinElmer Life and Analytical Sciences, Boston, MA). Aliquots of feces homogenate (0.05-0.15 g) was mixed with Soluene-350 in a 25-mL glass scintillation vial and was incubated overnight with gentle shaking in a 60°C water bath. Upon cooling, 0.2 mL of 30% hydrogen peroxide and 15 mL Ecolite™ were added. The vial was kept in the liquid scintillation counter for 1 or 2 days before counting.

**HPLC/MS/MS Analysis.** HPLC analysis was performed on an Agilent 1100 series HPLC system (binary pump, autosampler, and an adjustable wavelength UV detector). Samples were injected onto a YMC ODS AQ reversed phase column (4.6 x 150 mm, 5 μ, YMC, Japan) and separated in 75 min at a flow rate of 1.0 mL/min using mobile phases consisting of 0.06% TFA in water (solvent A) and 0.06% % TFA in acetonitrile (solvent B). The solvent gradient was as follows: 5% to 25% B in 5 min, 25% to 40% B in 15 min, 40% to 53% B in 40 min, 53% to 60% in 3 min, 60% to 90% in 2 min, 90% B for 7 min, 90% to 5% B in 3 min. The HPLC eluent went through a splitter so that 25% of the eluent was subjected to MS/MS analysis with a Finnigan LTQ ion trap mass spectrometer (ThermoFinnigan, San Jose, CA) using electrospray ionization (ESI) in the positive ion mode. The remaining 75% of the eluent was collected into Luma plates®-96 (PerkinElmer Life and Analytical Sciences, Boston, MA) at 0.26-min intervals using a Gilson FC 204 96-well fraction collector (Gilson Medical Electronics, Middletown, WI) for radioactivity determination.

**Accurate Mass Analysis**.  Pooled bile samples were analyzed by HPLC with Shimadzu LC-10AD binary pumps (Shimadzu, Kyoto, Japan) equipped with a LEAP auto-sampler on an YMC ODS AQ column (2.0x50 mm, 5 μ). The flow rate was 300 μL/min. Solvent B was maintained at 0% for 0.5 min, then increased to 70% in 15 min, then to 90% in 0.5 min, then maintained at 90% for 2 min. For accurate LC/MS analysis, the HPLC eluent was directed to a Micromass Q-TOF API-US mass spectrometer that was equipped with a Lock-Spray and an ESI source (Waters, MA) and analyzed in the positive ion mode. An infused solution

DMD 7856

of a compound with a formula of $C_{38}H_{53}N_6O_7$ was used to provide the Lock Mass (m/z 705.3976). The Q-TOF was tuned to 18,000 resolution at half peak height of the reference compound.

**Radiochromatographic Analysis.** HPLC fractions collected in 96-well plates (Luma plates®-96) were dried in an Automatic Environmental Speed Vac (Savant, Holbrook, NY). Each well was then counted for radioactivity for 10 min using a Microplate Scintillation and Luminescence TopCount Counter (model NXT, Packard Instrument Company, Meriden, CT). For preparation of biotransformation profiles (radiochromatograms), a background count of 2-3 CPM was subtracted from the CPM value of each fraction. The resulting net CPM values were plotted against time-after-injection using Microsoft® Excel software. The relative distribution of each metabolite in a biotransformation profile was determined by summing of the radioactivity in the fractions corresponding to the metabolite divided by the total radioactivity collected during the entire HPLC run.

**Synthesis of M24:** 1-[3-(Dimethylamino)propyl]-3-ethylcarbodiimide hydrochloride (100 mg, 0.5 mmol) was added slowly to an ice-cold solution of muraglitazar (200 mg, 0.387 mmol), taurine (2-amino ethanesulfonic acid, 48.4 mg, 0.387 mmol), 1-hydroxybenzotriazole (67.7 mg, 0.5 mmol), and *N*-methyl morpholine (0.1 mL, 1 mmol) in dimethyl formide (2 mL) at 0°C. The reaction mixture was stirred at room temperature for 3 h. The reaction mixture was neutralized with aqueous HCl (0.2 mL of a 12 N solution) and was then purified directly by preparative HPLC (continuous gradient from 70%A:30% B to 0%A:100%B [A = 90% $H_2O$/10% MeOH + 0.2% TFA; B = 10% $H_2O$/90% MeOH +

DMD 7856

0.2% TFA] at a flow rate of 30 mL/min for 30 min on a Phenomenex LUNA 5 μ

C18(2) 30 x 250 mm column; detection at 220 nm) followed by lyophilization from

water to give the compound (155 mg, yield 64%). NMR analysis was performed

on a Joel 400 MHz spectrometer in chloroform-$d$. Proton chemical shifts are

reported in ppm relative to tetramethylsilane. MS (+ESI), [M + H]$^+$: 624, MS

fragments: m/z 292, 186, 416. $^1$H NMR (CDCl$_3$; 400 MHz) δ: 2.53 (CH$_3$, s), 2.93

(CH$_2$, bs), 3.19 (CH$_2$, bs), 3.61 (CH$_2$, bs), 3.73 (CH$_3$, s), 3.88-4.10 ( CH$_2$, d,

J=28Hz), 4.29 (CH$_2$, bs), 4.40-4.60 (CH$_2$, d, J=40Hz), 6.70-6.79 (2 aromatic-H, d,

J=10 Hz), 6.85 (2 aromatic-H, bs), 6.98-7.05 (2 aromatic-H, d, J=10Hz), 7.15-

7.25 (2 aromatic-H, d, J=5Hz), 7.30-7.50 (N-H, d, J=28Hz), 7.55-7.60 (2

aromatic-H, t, J=10Hz), 7.64-7.70(aromatic-H, t, J=10Hz), 8.11-8.12 (2 aromatic-

H, d, J=5Hz), 8.26 (1 acid-H, bs).

## RESULTS

**Excretion and Recovery of Administered Dose.** After a single oral dose of

[$^{14}$C]muraglitazar, the majority of radioactivity was recovered in feces of intact

mice (approximately 80% of dose) and bile of BDC mice (>65% of dose) over a

0-24 hour collection period (Table 1). Urine contained 7-16% of the administered

dose. In group 1M (1 mg/kg dose, intact mice), 87% of the dose was recovered in

excreta in the first 24 hours after administration, while greater than 90% of the

dose was excreted in the same period in the other three groups. Therefore, the

fecal route via biliary excretion was the major elimination pathway for

[$^{14}$C]muraglitazar in mice.

13

**Metabolite Profiles**. Distribution of [$^{14}$C]muraglitazar and its metabolites in plasma at 1, 4, 12, and 24 h is presented in Table 2. Distribution of muraglitazar and its metabolites in feces of intact mice and bile of BDC mice, as the major elimination route, is presented in Table 3. Representative radiochromatograms for plasma, urine, feces, and bile samples from group 2M or 4M are shown in Figure 2.  The parent compound was the minor component in bile, feces, and urine samples, indicating that muraglitazar was extensively metabolized in mice.

**Plasma.** The concentrations of total radioactivity in plasma (µg equivalents of muraglitazar per mL plasma) at 1, 4, 12, and 24 h were 2.6, 1.7, 0.15, and 0.03 for group 1M, and 78.6, 79.1, 3.4, 3.0 for group 2M, respectively. Plasma samples at 1 h were similar to those at 4 h and contained 10-25 fold higher total radioactivity than those plasma samples at 12 h and 24 h. The total radioactivity in 12 h and 24 h samples were comparable. Therefore, similar to that in other species, the total radioactivity appeared to reach the maximum concentration at 1 h and the exposure to the parent compound was proportional to doses. Metabolite profiles in plasma for both 1 mg/kg and 40 mg/kg dose groups were similar. The parent compound represented the major radioactive peak in all plasma samples. M18b (glucuronide conjugate of hydroxy muraglitazar) was a trace metabolite at 1 h and a minor metabolite at 4 h. At 12 and 24 h, the level of M18b became comparable to that of the parent drug and M34, a dehydrogenated metabolite, was evident as a minor metabolite. Three trace metabolites, M11, M14 and M24, were detected only by LC/MS in the 24 h plasma of the 40 mg/kg dose group.

**Bile.** The major portions of radioactive dose (>65%) were found in the bile at both 1 and 40 mg/kg doses (Table 1) and the parent compound only accounted for <4% of dose (Table 3). The metabolite profiles of bile were similar between the 1 and 40 mg/kg doses. Taurine conjugates M24 and M26(a,b,c), hydroxy metabolite M10, glucuronide conjugate M13, *O*-dealkylated metabolites M1 and M21, and the parent drug were prominent components in mouse bile. In addition, radioactive peaks corresponding to M4, M7, M9, M11, M12, M14, M15, M16, M18(a,b,c), M25, M27, M28, M29(a,b), M30, M31, M32, M33 and M35 were visible in the HPLC radiochromatogram (Figure 2). Metabolite M2, M5, M6, M8, M8a, M17, M20, M26(d,e) and M34 were detected by LC/MS/MS in trace amounts in the 40 mg/kg dose group.

Metabolite M24, a taurine conjugate, was the most abundant drug related species in the bile, and accounted for 12.4% and 15.1% of the total dose for the 1 mg/kg and 40 mg/kg dose groups, respectively. The total amount of taurine conjugates (M24, M25, M26a,b,c, and M31) accounted for 20.8% and 21.6% of the dose at 1 mg/kg and 40 mg/kg. Three glutathione conjugates, M29a, M29b, and M30, accounted for 3.3, 0.8, and 1.8% of the dose at 1 mg/kg and 1.8, 0.9, and 1.1% of the dose at 40 mg/kg.

**Feces.** The major portions of the radioactive doses (>80%) were found in feces of intact mice (groups 1M and 2M) and a small portions of radioactive doses (<12%) were found in feces of BDC mice (group 3M and 4M). Radioactivity was distributed among M1, M8a, M9, M10, M11, M12, M14, M15, M16, M21, M24, M26(b,c), M27, M28, M32, M33, and muraglitazar in the fecal samples of intact

mice. M1, M9, M10, M24, and muraglitazar were the major components in groups 1M and 2M. In addition, M3, M5 and M7 were detected by LC/MS as trace metabolites in the 40 mg/kg dose group.

M1, M9, M10, M12, M13, M14, M15, M18g, M20b, M21, M27, M28, and muraglitazar were the most prominent components in the fecal samples of BDC mice (groups 3M and 4M). The taurine conjugates, M24 and M26(a,b), were not detected in the fecal samples from BDC mice of either dose group.

M1 and M21 appeared to be the major metabolites in the feces of BDC mice, but the minor metabolites in the feces of intact mice; however, these metabolites represented similar percent of doses between the BDC and intact mice.

**Urine.** Urine represented a minor elimination pathway for [$^{14}$C]muraglitazar. The predominant radioactive metabolites in the urine samples were M1 and M21 for all groups. The parent drug was a trace component in all mouse urine samples. M10, M12, M14, M17b, M18b, M24 were detected only by LC/MS in the 40 mg/kg dose group.

**Identification of Metabolites.** More than thirty metabolites were found in mice following oral administration of [$^{14}$C]muraglitazar. M1-M21 have been previously identified in humans following oral administration of [$^{14}$C]muraglitazar (Table 4) (Wang et al., 2005, Zhang et al., 2005). These metabolites were assigned in this study by comparing retention time, MS/MS fragmentation and relative elution order with previously identified metabolites. Multiple isomers (the same molecular weight but different HPLC retention times and/or MS/MS patterns) were detected for acyl glucuronides (M13, M17, M18 and M20), which may result from acyl

16

migration and/or different hydroxylation positions (in the case of M17 and M18).

Each isomer of these conjugates with the same molecular weight was assigned a

unique metabolite number and letter designation. Multiple acyl migration isomers

including M13a-d, M17a-j, M18a-g, and M20a-e (Table 4) were observed in

LC/MS/MS analysis of mouse bile in this study. The structures of these acyl

migration isomers were not further elucidated. The acyl migration isomers of

glucuronide metabolites were not observed in human bile sample (Wang et al.,

2005).

Metabolites M24-M35 were not detected in humans, monkeys or rats following

single oral doses of [$^{14}$C]muraglitazar (Zhang et al., personal communication).

Their structural assignments in this study were based on the MS/MS

fragmentation patterns (Table 4) and comparison to an authentic standard of

M24. The MS/MS fragmentation pattern of muraglitazar ([M+H]$^+$ = 517) showed

cleavage adjacent to the carbamate nitrogen (C3-N) to give a fragment at m/z

292 (relative intensity 90%) and cleavage at the alkyl ether bond (C8-O) to give a

fragment at m/z 186 (relative intensity 100%).  The two cleavage points divided

the molecule into three moieties: A, B, and C (Figure 1).

**M24**: M24 had a molecular ion at m/z 624 (equivalent to parent + 107) and two

major MS/MS fragment ions (m/z 292 and 186) similar to those of muraglitazar

(Figure 3), suggesting that modification occurred at the carboxylic acid side of the

molecule. Accurate mass analysis indicated that the metabolite had an empirical

formula of C31H33N3O9S (Table 5), which suggested that the modification

resulted in the addition of a sulfur and a nitrogen atom. M24 was tentatively

identified as the acyl taurine conjugate of muraglitazar. Thus, fragment ions at m/z 542 (624-82), m/z 499 (624-125) and m/z 471 (624-153) were proposed to result from the loss of $H_2SO_4$, taurine ($H_2NC_2H_4SO_3H$), and HC(O)-taurine (HC(O)NHC$_2$H$_4$SO$_3$H), respectively (Figure 3). The taurine conjugate standard, BMS-732106 (Figure 1), was subsequently prepared through chemical synthesis and subjected to full structural characterization. In addition to the same MS/MS patterns, coinjection of BMS-732106 and the bile sample showed that M24 and BMS-732106 had identical retention times, which confirmed the structural assignment of M24.

**M25**: M25 had a molecular ion at m/z 610 (equivalent to parent -14 +107) and two major MS/MS fragment ions (m/z 292 and 186) (Figure 3). Accurate mass analysis suggested that this metabolite had an empirical formula of C30H31N3O9S (Table 5), which suggested that the modification resulted in the addition of a sulfur and a nitrogen atom. Thus, the structure of M25 was proposed to be the taurine conjugate of *O*-demethyl muraglitazar.

**M26**: Five metabolites with a molecular ion at m/z 640 (equivalent to parent +16+ 107) were detected in bile and assigned as M26a, M26b, M26c, M26d and M26e. The structures of the five isomers were proposed to be taurine conjugates of hydroxy muraglitazar. The key MS/MS fragments ions (Table 4, Figure 4) for these metabolites were: m/z 308 (292+16) and 187 for M26a, m/z 290 (292+16-18) and 187 for M26b, m/z 290 (292-2) and 202 (186+16) for M26c, m/z 432, 292 and 186 for M26d, and m/z 202 (186+16) and 308 (292+16) for M26e. These

data suggested that M26a, b, c, e had the hydroxyl groups on moiety A, while M26d had the hydroxyl group on moiety C.

**M27 and M28**: M28 had a molecular ion at 535 (equivalent to parent + 18) and a corresponding fragment ion of m/z 204 (186+18), suggesting addition of $H_2O$ to moiety A. A proposed structure for M28 was shown in Figure 5. M27 had a molecular ion at m/z 537 (equivalent to parent +18+2) and a fragment ion at m/z 206 (186+18+2), suggesting addition of $H_2O$ and two hydrogen atoms to moiety A. M27 was proposed to be formed *via* reduction of M28.

**M30**: M30 had a molecular ion at m/z 840 (equivalent to parent+16+307), suggesting addition of an oxygen atom, one hydrogen, and the elements of glutathione (GSH). Accurate mass analysis supported such a structure with a proper empirical formula. The glutathione conjugation structure was supported by two characteristic mass fragment ions at m/z 711 (840-129) and 765 (840-75), resulting from the loss of $\gamma$-glutamyl and glycine moieties of glutathione, respectively (Figure 6) (Baillie *et al.*, 1993; Jin *et al.*, 1994). Fragment ions at m/z 615 (840-225), 597 (840-18-225), and 468 (840-18-225-129) suggested that the modification was not on moiety C (neutral loss of moiety C: 225). The fragmentation pattern (Figure 6) of the predominant fragment ion, m/z 308, suggested that it was a mixture of protonated glutathione ion ([GSH+$H^+$, m/z 308] and a daughter ion of m/z 840 after loss of GSH and moiety C (840-307-225). Thus, the fragment ions of m/z 179 (308-129), 162 (308-146) and 233 (308-75) were proposed to be derived from the protonated glutathione ion, while fragment ions of m/z 187 and 265 were proposed to be derived from the fragment ion of

m/z 308 (840-307-225). These data indicated that glutathione was readily removed from the molecular ion of M30, consistent with an attachment of the glutathione to moiety A or B. Thus M30 was proposed as hydroxy glutathionyl muraglitazar (Figure 6).

**M29a,b**: M29a and M29b had molecular ions at m/z 856 (equivalent to parent +16+307+16), indicating addition of 16 (one oxygen atom) to the molecular weight found for M30. M29a and M29b were proposed to be isomers of dihydroxy glutathionyl muraglitazar. Fragment ions of M29a at m/z 709 (856-18-129), 691 (856-18-18-129) and 745 (856-18-18-75) gave support for the assignment of this glutathione adduct (Figure 7). The fragment ion of m/z 595 (856-18-18-225) indicated that the glutathione was not on moiety C, while the fragment ion of m/z 290 (292+16-18) suggested that at least one hydroxyl group was on moiety A. The major fragment at m/z 515 (856-18-18-305) indicated that M29a lost the glutathione and the two water molecules simultaneously, which suggested that the glutathione was not on either phenyl rings of the moiety A or B. On the contrary, the fragment ion at m/z 409 may be attributed to an attachment of glutathione to phenylcyanide, implying that glutathione might attach to the phenyl ring of the moiety A. Thus, position of the glutathione group was not further defined.

The structural assignment of M29b as a glutathione adduct was supported by fragment ions at m/z 709, 691 and 763 (856-18-75) (Figure 8). Fragment ions of m/z 613 (856-18-225) and 484 (856-18-225-129) indicated that the glutathione was not on moiety C while fragment ion of m/z 290 (292+16-18) suggested that

DMD 7856

at least one hydroxyl group was on moiety A. Accurate mass analysis of M29b

provides additional support to the assignment with a proper empirical formula

(Table 5). Therefore, M29a and M29b might be positional isomers of dihydroxy

glutathionyl muraglitazar.

**M31**: M31 had a molecular ion at m/z 656 (equivalent to parent+32+107),

consistent with dioxygenation plus taurine formation. Fragment ions at m/z 306

(292+32-18) and 218 (186+32) suggested that both the added oxygen atoms

were on moiety A and at least one oxygen atom was attached to  a carbon that

yielded the corresponding water loss in the m/z 306 fragment ion. M31 was

identified as a taurine conjugate of a dihydroxy muraglitazar derivate with both

hydroxyl groups on moiety A (Figure 5).

**M32**: M32 had a molecular ion at m/z 549 (517+32), consistent with

dihydroxylation (Figure 5). M32 showed fragment ions at m/z 306 (292+32-18),

218 (186+32), and 187. Based on these fragment ions, the addition of both

hydroxyl groups was on moiety A.

**M33** and **M35**: These two metabolites had the same molecular ion at m/z 533

(517+16), indicating mono-oxidation. Both metabolites showed fragment ions at

m/z 308 (292+16) and 186, suggesting that the hydroxyl group was not located

on moiety A and rather on moiety B (Figure 5).

**M34**: M34 had a molecular ion at m/z 515 and a major MS/MS fragment at m/z

290, suggesting that it had lost two hydrogen atoms and the modification

occurred on moiety A or B. The only plausible site for this transformation was

between C-8 and C-9. M34 eluted after muraglitazar in the reversed phase HPLC

system, which makes it unlikely that the m/z 515 ion resulted from dehydration of a hydroxy muraglitazar derivative (m/z 533) in the ionization source. Therefore, M34 was identified as an 8-ene muraglitazar derivative (Figure 5).

**LC/MS Profiles of Taurine and Glutathione Conjugates in Bile Samples From Other Species**

The finding of taurine and glutathione conjugates in mouse samples prompted investigation of whether these previously unidentified metabolites were present in other species. Bile samples of rats (20 mg/kg dose), monkeys (2 mg/kg dose) and humans (10 mg/subject) following oral administration of [$^{14}$C]muraglitazar from previous studies were re-analyzed with LC/MS methods used in this study. Figures 9 and 10 show LC/MS ion chromatographic profiles of glutathione conjugates M29 (a,b) and M30 in bile samples of mice, rats, monkeys, and humans following oral administration of [$^{14}$C]muraglitazar. None of the taurine or glutathione conjugates found in this study with mouse samples were detected in bile samples of rats, monkeys and humans.

**DISCUSSION**

The metabolism of muraglitazar was determined in intact and BDC male CD-1 mice. The work was done in order to compare the metabolite profiles in mice to those previously determined in humans (Wang et al., 2005, Zhang et al., 2005). The excretion profile for [$^{14}$C]muraglitazar was similar between the low and high dose groups (Table 1). In addition, the metabolic profiles were similar for both groups in all matrices (bile, feces, plasma and urine). These data suggested that

DMD 7856

there were no metabolism or disposition pathways saturated over this dose range.

After oral administration of [$^{14}$C]muraglitazar, the major drug-related circulating component was the parent compound for up to 4 h post dose at both 1 and 40 mg/kg. Both the parent compound and the ether glucuronide of hydroxy muraglitazar, M18b, were the major components at 12 and 24 h post dose. *O*-Dealkylated metabolites, M1 and M21, were the major metabolites in the mouse urine, however, urinary excretion was relatively minor. Biliary elimination of metabolites and the parent drug was the major clearance pathway at both low (1 mg/kg) and high (40 mg/kg) doses. This overall elimination profile was similar to what was observed in humans (Wang et al., 2005, Zhang et al., 2005) and monkeys and rats (Zhang et al., personal communication). However, the metabolite profiles of bile and feces of mice were quite different from those of other species. M24, the taurine conjugate of muraglitazar, was found to be the most abundant metabolite, accounting for 12-15% of the dose in the bile of BDC mice or 7-12% of the dose in the feces of intact mice without bile collection. M13, the acyl glucuronide of muraglitazar, the most abundant drug related species in human bile, was also a major metabolite in mouse bile, but was not present in mouse feces. The acyl glucuronide was presumably hydrolyzed in the intestinal tract after biliary excretion. M10, a hydroxylated metabolite, was another major metabolite in mouse bile, although it was a minor metabolite in bile samples from other species.

In addition to those metabolite found in other species, several unique metabolites were found in mice (Figure 5). Among them, a series of taurine conjugates (M24, M25, M26a,b,c,d,e and M31) were found that accounted for more than 20% of the total administered dose for both the 1 mg/kg and 40 mg/kg groups. These metabolites were present at high levels in bile and feces, and were also detected in plasma and urine. The formation of taurine or glycine conjugates of bile acids is known to proceed *via* a two-step enzymatic reaction in liver (Lim et al, 1981). The first step is catalyzed by acyl-CoA synthase, which converts bile acids to their respective acyl-CoA thioester. Bile acid-CoA:amino acid *N*-acyltransferase then transfers the acyl group to taurine or glycine to form the corresponding conjugates (Falany, 1994). The taurine conjugates of muraglitazar and its oxidative metabolites found in this study are presumably formed *via* acyl-CoA thioester intermediates as demonstrated for the formation of taurine conjugates of other xenobiotic carboxylic acids (Fears et al., 1985). The large amounts of taurine conjugates of muraglitazar in mice suggested that acyl-CoA synthases and acyltransferases in the mouse liver have the ability to utilize muraglitazar and its oxidative metabolites as substrates quite efficiently, while the taurine conjugating enzymes in other species are not able to catalyze these reactions. Interestingly, the glycine conjugate of muraglitazar was not detected, which might be due to a change in relative rate of formation of glycine *vs*. taurine conjugates with different acid structures as has been suggested by Czuba et al (Czuba et al., 1982).

The glutathione adducts M30 and M29a,b are the second set of related metabolites that are unique to mice. These glutathione adducts were detected at very low levels only in mouse bile from the 40 mg/kg group and they were not found in other species following oral administration of muraglitazar (Figure 10). Thus any possible biological/toxicological effect implicated by formation of these metabolites should also be unique to mice. These glutathione conjugate metabolites showed characteristic GSH conjugate fragmentation patterns upon LC/MS/MS analyses. The glutatione adduct detected with muraglitazar could be explained by an epoxidation of the oxazole ring of muraglitazar followed by a nucleophilic attack on the epoxide by glutathione (Figure 11).

There are multiple mechanisms that could be postulated for the formation of M28, however, the most straightforward mechanism is through direct enzymatic hydrolysis. Electron-deficient carbon atoms in the oxazole ring can undergo nucleophilic/hydrolysis reactions. The enzymatic hydrolysis of an oxazole-contaning compound to generate a ring opened product has been described previously (Balani *et al.*, 1994). It is plausible that the methyl ketone group in M28 would be reduced by an oxidoreductase to give M27. The carbonyl reduction by a cytosolic keto-aldo reductase provided an example for this conversion of M28 to M27 (Martin et al., 2005). Elution order of the two metabolites in the reversed phase column indicated that M27 was more polar than M28, which was consistent to proposed structures of M27 and M28.

The major site of hydroxylation of muraglitazar in humans occurred on moiety A (Zhang et al., 2005). The fragment ion of m/z 187 with an empirical formula of

25

DMD 7856

$C_{12}H_{11}O_2$ was observed previously for M8a, M10, and M14. This fragment was postulated to be formed through a gas-phase replacement of a nitrogen atom with an oxygen atom after ether cleavage of the oxygenated fragment (187=186-NH+oxygen) in the mass spectrometer (Zhang et al*.,* 2005). Alternatively, cleavage at the C3-N bond adjacent to the carbamate group and loss of phenyl cyanide from moiety A would also result in a fragment ion at m/z 187. A phenyl cyanide would be formed through a reverse Diels-Alder reaction in the gas phase of the mass spectrometer. The product ion of m/z 187 was characteristic to those metabolites with hydroxylation sites at C8, C9, or C12 such as M10, M14, and M8a, but was not seen in the parent or in other hydroxylated metabolites. Mouse CYP enzymes seemed to exhibit different regio-selectivity, as hydroxylation was also observed on both moiety B (M33 and M35) and moiety C (M26d). There are three possible hydroxylation sites on moiety B: C-3, C-5 and C-6. The low intensity ratio of fragment ions at m/z 186 to m/z 308 (about 1/10) for M35 indicated that carbamate cleavage was much easier than ether cleavage in M35 for this metabolite, possibly due to weakening of the C-N bond by resonance effects of a OH group at C-3 or C-5. On the other hand, M33 showed a "normal" intensity ratio of fragment ions at m/z 186 to m/z 308 (2/1), and suggested that the C-N bond was similar to that in muraglitazar, which would localize the OH group to C-6.

The isomerization *via* acyl migration observed in this study was likely due to the conditions employed for the sample collection. Mouse bile was acidified upon thawing by the addition of glacial acetic acid to a final concentration of 2% (v/v) in

DMD 7856

the present study. The acyl glucuronide of muraglitazar and its metabolites showed evidence of acyl migration to multiple isomers. This behavior was not observed in the previous studies in human bile (Wang *et al.*, 2005). As those studies were done with the addition of 5% (v/v) glacial acetic acid upon bile sample collection, it is concluded that the present protocol used for the mouse bile did not provide sufficient pH control and that the acyl migration found in this study was due to *ex vivo* effects. Acyl migration is known to be pH and temperature dependent (Sallustio *et al.*, 2000). The results highlight the importance of proper sample collection and storage procedures for prevention of *ex vivo* acyl migration.

The full characterization of the biotransformation profile of drug candidates is not often conducted in mice. The fact that mouse is often a pharmacological model for many drug candidates and is also a species used for carcinogenicity study provides justification for the determination of the biotransformation profile of a new chemical entity in mice. As we learned from this study, the mouse generated all the metabolites found in the human and rat following administration of [$^{14}$C]muraglitazar, as well as several additional metabolites not previously identified in the other species.

In summary, muraglitazar was the major drug-related circulating component in mice after oral administration. Fecal excretion *via* biliary elimination was the major elimination pathway for [$^{14}$C]muraglitazar. However, the major metabolic pathway of muraglitazar in mice was taurine conjugation. Additional metabolic pathways were similar to those found in humans including glucuronidation,

27

DMD 7856

hydroxylation, O-dealkylation, and a combination of these modifications. The taurine conjugate was demonstrated to be a unique metabolic pathway of muraglitazar in mice.

## ACKNOWLEDGEMENTS

# REFERENCE

Baillie TA and Davis MR (1993) Mass spectrometry in the analysis of glutathione conjugates. *Biol Mass Spectrom* **22**:319-25.

Balani SK, Kauffman LR, Arison BH, Olah TV, Goldman ME, Varga SL, O'Brien JA, Ramjit HG, Rooney CS and Hoffman JM (1994) Metabolism of 3-[2-(benzoxazol-2-yl)ethyl]-5-ethyl-6-methylpyridin-2 (1H)-one (L-696,229), an HIV-1 reverse transcriptase inhibitor, by rat liver slices and in humans. *Drug Metab Dispos* (1994) **22**:200-205.

Czuba B and Vessey DA (1982) The effect of bile acid structure on the activity of bile acid-CoA:glycine/taurine-N-acyltransferase. *J Bio Chem* **257**:8761-8765.

Devasthale PV, Chen S, Jeon Y, Qu F, Shao C, Wang W, Zhang H, Cap M, Farrelly D, Golla R, Grover G, Harrity T, Ma Z, Moore L, Ren J, Seethala R, Cheng L, Sleph P, Sun W, Tieman A, Wetterau JR, Doweyko A, Chandrasena G, Chang SY, Humphreys WG, Sasseville VG, Biller SA, Ryono DE, Selan F, Hariharan N and Cheng PTW (2005) Design and synthesis of *N*-[(4-methoxyphenoxy)carbonyl]-*N*-[[4-[2-(5-methyl-2-phenyl-4-oxazolyl)ethoxy] phenyl]methyl]glycine, muraglitazar /BMS-298585], a novel peroxisome proliferator-activated receptor r/γ dual agonist with efficacious glucose and lipid-lowering activities. *J Med Chem* **48:** 2248-2250.

Falany CN, Johnson MR, Barnes S, and Diasio RB (1994) Glycine and taurine conjugation of bile acids by a single enzyme. Molecular cloning and expression of human liver bile acid CoA:amino acid N-acyltransferase. *J Biol Chem* **269**:19375-19379.

Fears R (1985) Lipophilic xenobiotic conjugates: The pharmacological and toxicological consequences of the participation of drugs and other foreign compounds as substrates in lipid biosynthesis. *Prog Lipid Res* 2**4**:177-195.

Jin L, Davis MR, Hu P, and Baillie TA (1994) Identification of novel glutathione conjugates of disulfiram and diethyldithiocarbamate in rat bile by liquid chromatography-tandem mass spectrometry. Evidence for metabolic activation of disulfiram in vivo. *Chem Res Toxicol* **7**:526-33.

Lim WC and Jordan TW (1981) Subcellular distribution of hepatic bile acid-conjugating enzymes. *Biochem J* **197**: 611-618.

Martin HJ, Ursula Breyer-Pfaff U, Wsol V, Venz S, Block S, and Maser E (2006) Purification and characterization of AKR1B10 from human liver: role in carbonyl reduction of xenobiotics. *Drug Metab Dispos* Published December 28, 2005; doi: 10.1124/dmd.105.007971.

Sallustio BC, Sabordo L, Evans AM, and Nation RL (2000) Hepatic disposition of electrophilic acyl glucuronide conjugates. *Current Drug Metab* **1**:163-180.

Wang L, Zhang D, Swaminathan A, Xue Y, Cheng PT, Mosqueda-Garcia R, Everett DE, and Humphreys WG (2005) Glucuronidation as a major metabolic

DMD 7856

clearance pathway of [$^{14}$C]muraglitazar in humans: Metabolic profiles in subjects with or without bile collection. *Drug Metab Dispos* **34:** Fast Forward.

Zhang D, Zhang H, Aranibar N, Hanson R, Huang Y, Cheng PT, Wu S, Bonacorsi S, Zhu M, Swaminathan A, and Humphreys WG (2006) Structural elucidation of human oxidative metabolites of muraglitazar: Use of microbial bioreactors in the biosynthesis metabolite standards. *Drug Metab Dispos* **34:** Published November 9, 2005; doi: 10.1124/dmd.105.007153.

## Legends of Figures

Figure 1.      Structures of muraglitazar and muraglitazar taurine conjugate M24, and their major MS/MS fragments.

Figure 2.      Representative HPLC-radiochromatograms of metabolites of [$^{14}$C]muraglitazar in mice after a 40 mg/kg oral dose (P = muraglitazar; 1, 2, 3, … = M1, M2, M3, …).

Figure 3.      Structures and MS/MS spectra of M24 and M25.

Figure 4.      MS/MS spectra of M26a, M26b, M26c, M26e and M26d.

Figure 5.      Proposed unique metabolic pathways of muraglitazar in mice. The structures were proposed based on LC/MS/MS analyses.

Figure 6.      Proposed structure and MS/MS spectra of M30 (one of the possible structures was shown in Figure 11).

Figure 7.      Proposed structure and MS/MS spectrum of M29a (one of the possible structures was shown in Figure 11).

Figure 8.      Proposed structure and MS/MS spectrum of M29b (one of the possible structures was shown in Figure 11).

Figure 9.      LC/MS ion chromatographic profiles of taurine conjugates M24 and M26 (b,c) in bile samples of mice (40 mg/kg dose), rats (20 mg/kg dose), monkeys (2 mg/kg dose), and humans (10 mg/subject dose) following oral administration of [$^{14}$C]muraglitazar.  Aliquots of bile samples (10-30 μl) were analyzed by LC/MS.

Figure 10.     LC/MS ion chromatographic profiles of glutathione conjugates M29 (a,b) and M30 in bile samples of mice (40 mg/kg dose), rats (20 mg/kg dose), monkeys (2 mg/kg dose), and humans (10 mg/subject dose) following oral administration of [$^{14}$C]muraglitazar. Aliquots of bile samples (10-30 μl) were analyzed by LC/MS.

Figure 11.     Proposed formation pathways for M27,  M28, M29a,b and M30. The metabolite structures presented in this Figure are proposed based on the limited LC/MS/MS analyses.

31

DMD 7856

Table 1.  Recovery of radioactivity in urine, feces and bile during the 0-24 hour collection period after a single oral dose of [$^{14}$C]muraglitazar to mice (data were obtained with pooled samples from each group

| Group | Dose (mg/kg) | Recovery of radioactivity (% dose) | | | |
|---|---|---|---|---|---|
| | | Urine | Feces | Bile | Total |
| 1M (intact mice) | 1 | 6.85 | 80.5 | - | 87.4 |
| 2M (intact mice) | 40 | 13.4 | 81.3 | - | 94.7 |
| 3M (BDC mice) | 1 | 8.26 | 8.17 | 74.8 | 91.2 |
| 4M (BDC mice) | 40 | 16.1 | 11.9 | 65.7 | 93.7 |

DMD 7856

Table 2. Distribution of muraglitazar and its metabolites in pooled plasma after a
single oral dose of [$^{14}$C]muraglitazar to mice

| Metabolites[a] | Relative distribution of metabolites (% of sample) | | | | | | | |
|---|---|---|---|---|---|---|---|---|
| | 1 mg/kg[b] | | | | 40 mg/kg[c] | | | |
| | 1 h | 4 h | 12 h | 24 h | 1 h | 4 h | 12 h | 24 h |
| Parent | 95.0 | 93.3 | 55.0 | 53.7 | 94.2 | 93.0 | 62.7 | 56.7 |
| M18b | Trace[e] | 2.5 | 37.7 | 46.3 | 0.8 | 3.0 | 29.9 | 33.8 |
| M34 | Trace | Trace | Trace | Trace | 0.3 | 0.3 | 4.3 | 6.6 |
| Other[d] | 5.0 | 4.2 | 7.3 | 0 | 4.7 | 3.7 | 2.9 | 2.9 |

[a] M11, M14, and M24 were trace metabolites detected by LC/MS only.

[b] Concentration of radioactivity in plasma (μg equivalents of muraglitazar /mL plasma) for 1, 4,
12, and 24 h were 2.6, 1.7, 0.15, and 0.03, respectively.

[c] Concentration of radioactivity in plasma (μg equivalents of muraglitazar /mL plasma) for 1, 4,
12, and 24 h were 78.6, 79.1, 3.4, and 3.0, respectively.

[d] Unidentified radioactivity.

[e] Detected by LC/MS but not by radioactivity.

Table 3.    Distribution of metabolites in feces of intact mice and bile of BDC mice (0-24 h) after a single oral dose of [$^{14}$C]muraglitazar

| Metabolites | Distribution of metabolites in feces of intact mice ( % of dose) | | Distribution of metabolites in bile of BDC mice ( % of dose) | |
|---|---|---|---|---|
| | 1M (1 mg/kg) | 2M (40mg/kg) | 3M (1 mg/kg) | 4M (40 mg/kg) |
| M1 | 7.1 | 6.2 | 2.3 | 1.5 |
| M4 | MD | ND | 2.3 | 1.8 |
| M5 | ND | Trace | ND | Trace |
| M7 | ND | Trace | 0.9 | 0.5 |
| M8 | ND | 2.0 | ND | Trace |
| M8a | ND | Trace | 0.5 | 0.4 |
| M9 | 12.9 | 6.6 | ND | Trace |
| M10 | 15.9 | 18.1 | 6.7 | 5.0 |
| M11 | ND | 1.7 | ND | Trace |
| M12 | 1.6 | 2.7 | 1.0 | 1.3 |
| M13a-d | ND | ND | 9.9 | 11.9 |
| M14 | 1.4 | 2.9 | 1.9 | 0.8 |
| M15 | 0.8 | 1.6 | 2.4 | 1.6 |
| M16 | ND | 1.0 | 0.1 | 0.1 |
| M17a-j | ND | ND | 1.7 | 0.7 |
| M18a-f | ND | ND | 3.6 | 1.7 |
| M20a-e | ND | ND | 1.3 | 0.8 |
| M21 | 3.3 | 2.9 | 4.1 | 3.1 |
| M24 | 12.3 | 7.2 | 12.4 | 15.1 |
| M25 | ND | ND | 2.9 | 0.7 |
| M26a-e | ND | 9.3 | 5.0 | 4.3 |
| M27 | ND | Trace | 3.4 | 1.8 |
| M28 | MD | 1.7 | 1.8 | 0.9 |
| M29a | ND | ND | 3.3 | 1.8 |
| M29b | ND | ND | 0.8 | 0.9 |
| M30 | ND | ND | 1.8 | 1.1 |
| M31 | ND | ND | 0.5 | 1.5 |
| M32 | MD | Trace | 1.6 | 0.9 |
| M33 | ND | Trace | Trace | Trace |
| M34 | ND | Trace | ND | Trace |
| M35 | ND | ND | Trace | Trace |
| Parent | 6.3 | 5.5 | 3.98 | 2.37 |
| Others | 19 | 11.9 | 0 | 1.8 |
| Total | 80.5 | 81.3 | 74.8 | 65.7 |

Others are not identified  peaks. ND = Not detected. Trace means detection by LC/MS but not by radioactivity.

Table 4. Muraglitazar metabolites identified in plasma, urine, bile and fecal
samples of  mice after a single oral dose of [$^{14}$C]muraglitazar

| Metabolite | Rt (min) | MH$^+$ | Major MS/MS Fragments [a] (ranked by intensity) | Proposed Identity |
|---|---|---|---|---|
| P | 63.24 | 517 | 186, 192 | Muraglitazar |
| M1 | 18.46 | 332 | 137, 107 | *O*-Dealkyl-muraglitazar |
| M2 | 22.04 | 519 | 308, 465, 483, 343,187 | 8-Hydroxy-*O*-demethyl-muraglitazar |
| M3 | 22.81 | 549 | 324, 187 | 8, 12-Dihydroxy-muraglitazar |
| M4 | 24.67 | 549 | 306, 425, 324, 187 | 9,12-Dihydroxy-muraglitazar |
| M5 | 25.28 | 519 | 290, 395, 447, 184 | 12-Hhydroxy-*O*-demethyl-muraglitazar |
| M6 | 27.43 | 519 | 202, 308 | 17-Hydroxy-*O*-demethyl-muraglitazar |
| M7 | 29.29 | 519 | 290, 202, 187 | 9-Hydroxy-*O*-demethyl-muraglitazar |
| M8a | 31.09 | 533 | 308, 202, 187 | 8-Hydroxy-muraglitazar |
| M8 | 32.42 | 549 | 306, 218, 324, 202 | 12, 17-Dihydroxy-muraglitazar |
| M9 | 34.18 | 507 | 529(Na)  to 282, 176 | Imide-derivative of muraglitazar |
| M10 | 36.21 | 533 | 409, 290, 187, 308, 205 | 12-Hydroxy-muraglitazar |
| M11 | 39.31 | 533 | 202, 308 | 17-Hydroxy-muraglitazar |
| M12 | 40.97 | 547 | 322, 216 | Muraglitazar 12-carboxylic acid |
| M13a | 39.98 | 693 | 292, 621, 557, 517 | Acyl glucuronide of muraglitazar |
| M13b | 41.28 | 693 | 517, 292 | Acyl glucuronide of muraglitazar |
| M13c | 43.23 | 693 | 292, 657, 613 | Acyl glucuronide of muraglitazar |
| M13d | 43.96 | 693 | 292, 657, 613, 583, 499 | Acyl glucuronide of muraglitazar |
| M14 | 42.56 | 533 | 202, 290, 308, 187 | 9-Hydroxy-muraglitazar |
| M15 | 44.87 | 503 | 186, 292 | *O*-Demethyl-muraglitazar |
| M16 | 50.23 | 549 | 594 (Me2NH) to 282, 176, 220 | N-Acetyl imide-derivative of muraglitazar |
| M17a | 20.79 | 695 | 519, 290 | Acyl glucuronide of hydroxy-*O*-desmethyl-muraglitazar |
| M17b | 21.26 | 695 | 519, 221 | Acyl glucuronide of hydroxy-*O*-desmethyl-muraglitazar |
| M17c | 22.75 | 695 | 659, 519, 290, 264, 308, 202 | Acyl glucuronide of hydroxy-*O*-desmethyl-muraglitazar |
| M17d | 24.26 | 695 | 519, 659, 637 | Acyl glucuronide of hydroxy-*O*-desmethyl-muraglitazar |
| M17e | 24.67 | 695 | 519 | Acyl glucuronide of hydroxy-*O*-desmethyl-muraglitazar |
| M17f | 25.08 | 695 | 519, 637, 558, 222 | Acyl glucuronide of hydroxy-*O*-desmethyl-muraglitazar |
| M17g | 26.2 | 695 | 519, 308, 202 | Acyl glucuronide of hydroxy-*O*-desmethyl-muraglitazar |
| M17h | 27.84 | 695 | 519, 202 | Acyl glucuronide of hydroxy-*O*-desmethyl-muraglitazar |
| M17i | 28.41 | 695 | 659, 519, | Acyl glucuronide of hydroxy-*O*-desmethyl-muraglitazar |
| M17j | 28.8 | 695 | 558, 659, 519 | Acyl glucuronide of hydroxy-*O*-desmethyl-muraglitazar |
| M18a | 23.35 | 709 | 533 | Acyl glucuronide of hydroxy-muraglitazar |
| M18b | 24.56 | 709 | 484, 378, 533, 308, 202 | Ether glucuronide of hydroxy-muraglitazar |
| M18c | 26.35 | 709 | 533, 290, 673, 307, 202 | Acyl glucuronide of hydroxy-muraglitazar |

| | | | | |
|---|---|---|---|---|
| **M18d** | 27.95 | 709 | 308, 673, 202, 290 | Acyl glucuronide of hydroxy-muraglitazar |
| **M18e** | 28.47 | 709 | 308, 202, 629, 673, 292 | Acyl glucuronide of hydroxy-muraglitazar |
| **M18f** | 29.96 | 709 | 290, 673, 202 | Acyl glucuronide of hydroxy-muraglitazar |
| **M18g** | 30.52 | 709 | 673, 290, 533, 202 | Acyl glucuronide of hydroxy-muraglitazar |
| **M20a** | 28.62 | 679 | 292, 503 | Acyl glucuronide of *O*-demethyl-muraglitazar |
| **M20b** | 30.99 | 679 | 292, 503, 643 | Acyl glucuronide of *O*-demethyl-muraglitazar |
| **M20c** | 39.78 | 679 | 292, 413, 621, 503, 263 | Acyl glucuronide of *O*-demethyl-muraglitazar |
| **M20d** | 40.3 | 679 | 292, 413, 503 | Acyl glucuronide of *O*-demethyl-muraglitazar |
| **M20e** | 41.07 | 679 | 292, 643, 413 | Acyl glucuronide of *O*-demethyl-muraglitazar |
| **M21** | 8.43 | 318 | 221, 177, 133, 199 | *O*-Dealkyl-*O*-desmethyl-muraglitazar |
| **M24** | 35.57 | 624 | 292, 186, 416, 499, 471, 542 | Taurine conjugate of muraglitazar |
| **M25** | 26.66 | 610 | 292, 186, 355 | Taurine conjugate of *O*-demethyl-muraglitazar |
| **M26a** | 19.74 | 640 | 308,519, 265 | Taurine conjugate of hydroxy-muraglitazar |
| **M26b** | 22.55 | 640 | 290,464, 308, 187 | Taurine conjugate of hydroxy-muraglitazar |
| **M26c** | 25.53 | 640 | 290, 202 | Taurine conjugate of hydroxy-muraglitazar |
| **M26d** | 27.02 | 640 | 432, 515, 292, 280, 186 | Taurine conjugate of hydroxy-muraglitazar |
| **M26e** | 23.4 | 640 | 202, 308, 464, 432 | Taurine conjugate of hydroxy-muraglitazar |
| **M27** | 25.89 | 537 | 206, 312, 238,188 | Reduction of hydration derivative of muraglitazar |
| **M28** | 32.78 | 535 | 204, 310, 186, 238 | Hydration derivative of muraglitazar |
| **M29a** | 13.78 | 856 | 820, 515, 709, 290, 691, 595, 533, 409 | Glutathione adduct of dihydroxy-muraglitazar |
| **M29b** | 15.86 | 856 | 709, 533, 290, 820, 691, 613 | Glutathione adduct of dihydroxy-muraglitazar |
| **M30** | 18.4 | 840 | 308, 693, 597, 711, 468, 765 | Glutathione adduct of hydroxy muraglitazar |
| **M31** | 18.98 | 656 | 306, 218 | Taurine conjugate of dihydroxy-muraglitazar |
| **M32** | 27.69 | 549 | 218, 306, 187 | Dihydroxy-muraglitazar |
| **M33** | 53.86 | 533 | 186, 308 | Hydroxy-muraglitazar |
| **M34** | 64.7 | 515 | 262, 290, 187 | 8-Ene-muraglitazar |
| **M35** | 47.6 | 533 | 308, 264, 186 | Hydroxy-muraglitazar |

[a] Major fragment ions for M9 and M16 were from their Na or $(CH_3)_2NH$ adduct ions, respectively. These adduct ions instead of their $MH^+$ were predominant species for these two metabolites.

DMD 7856

Table 5. Accurate mass determination of selected metabolites in bile of mice after a single oral dose of [$^{14}$C]muraglitazar.

| Metabolites | Formula | Calculated mass [M+H]$^+$ (m/z) | Observed mass [M+H]$^+$ (m/z) | Accuracy (ppm) |
|---|---|---|---|---|
| M24 | $C_{31}H_{33}N_3O_9S$ | 624.2016 | 624.1986 | -4.8 |
| M25 | $C_{30}H_{31}N_3O_9S$ | 610.1859 | 610.1906 | +7.8 |
| M26b | $C_{31}H_{33}N_3O_{10}S$ | 640.1965 | 640.1974 | +1.4 |
| M26c | $C_{31}H_{33}N_3O_{10}S$ | 640.1965 | 640.1955 | -1.6 |
| M27 | $C_{29}H_{32}N_2O_8$ | 537.2237 | 537.2197 | -7.4 |
| M28 | $C_{29}H_{30}N_2O_8$ | 535.2080 | 535.2053 | -5.0 |
| M29b | $C_{39}H_{45}N_5O_{15}S$ | 856.2711 | 856.2773 | +7.2 |
| M30 | $C_{39}H_{45}N_5O_{14}S$ | 840.2766 | 840.2791 | +3.0 |

# Figure 1



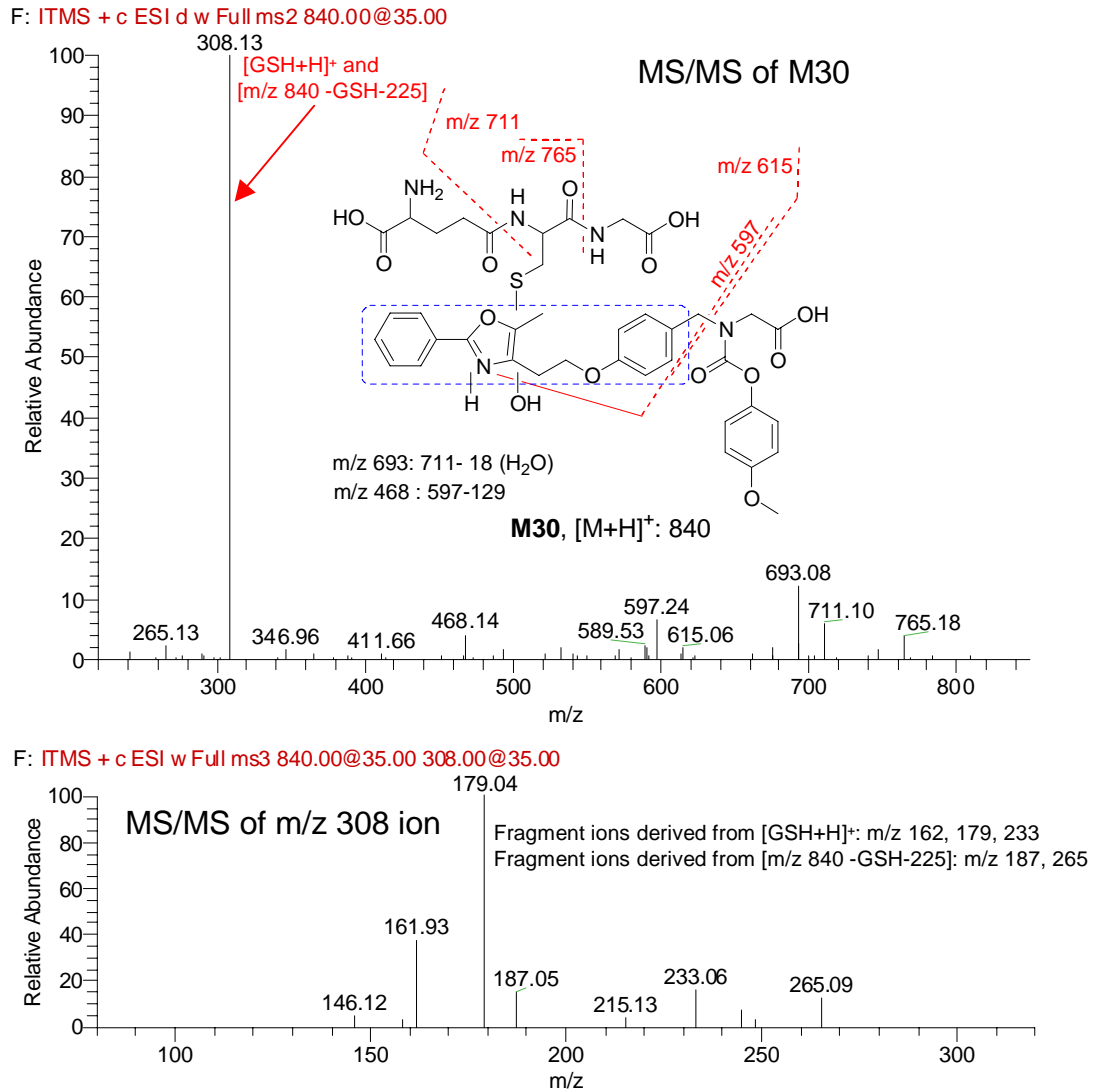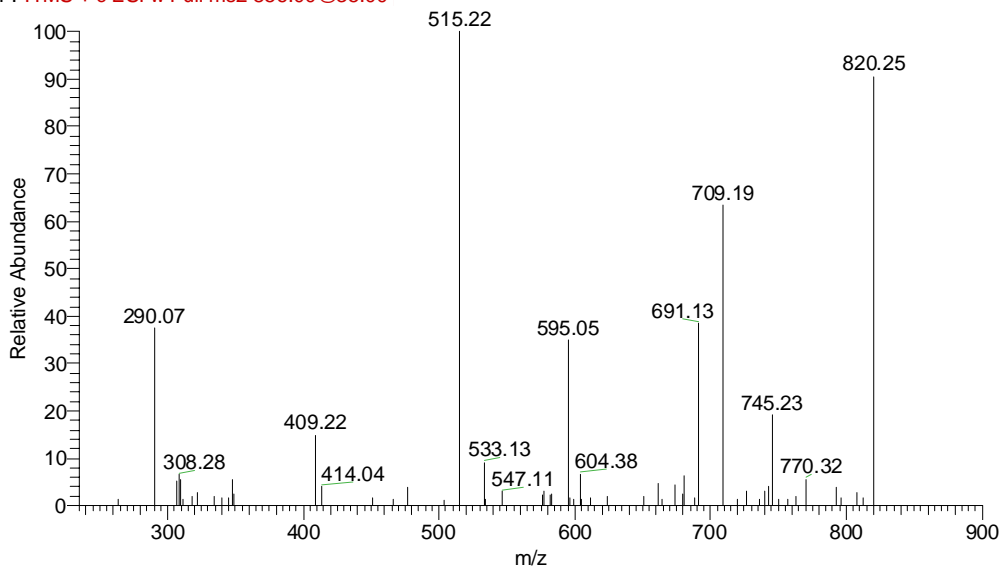muraglitazar, * denotes C-14 labeled carbons

M24
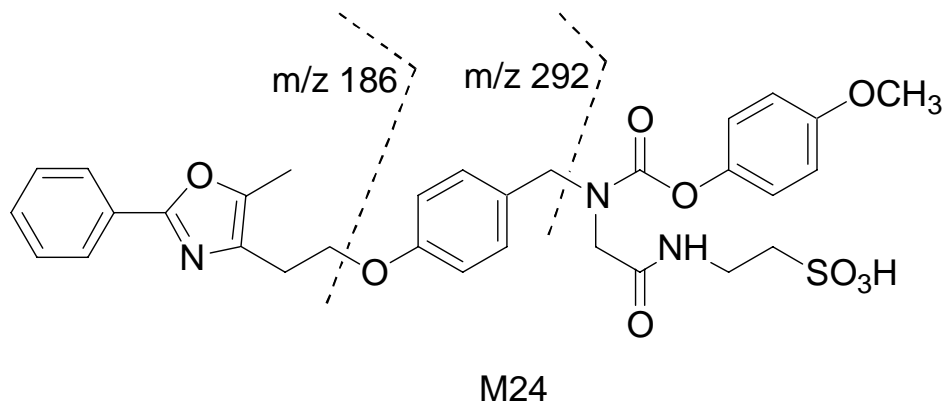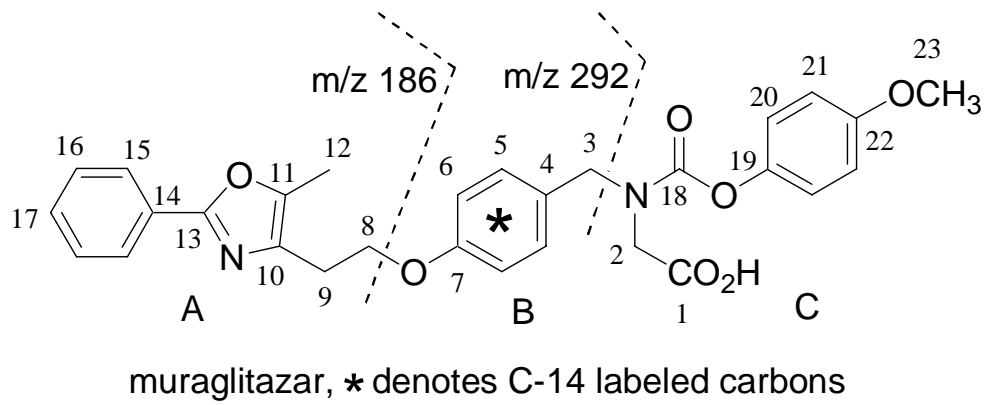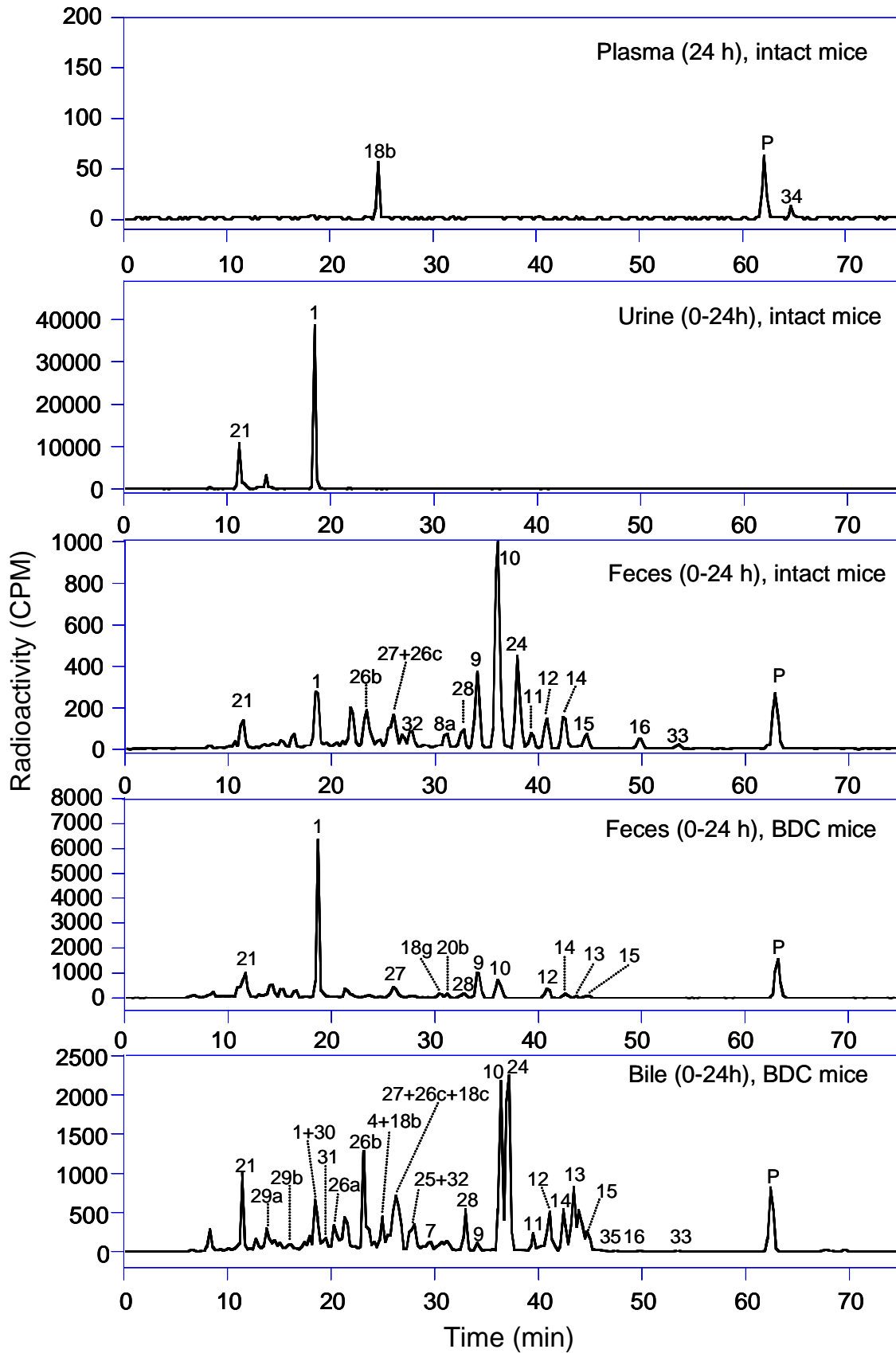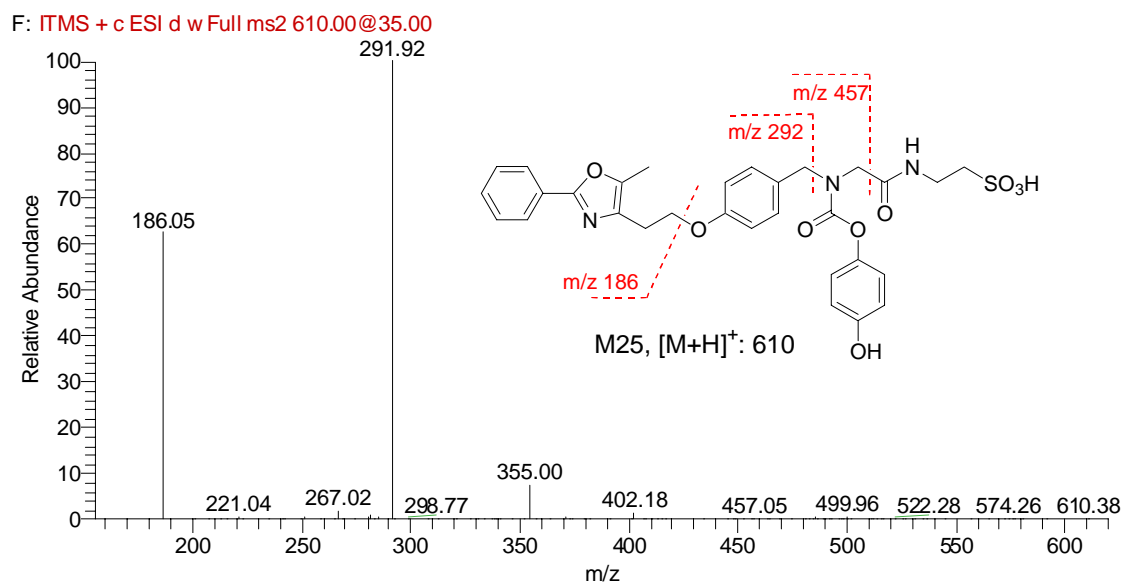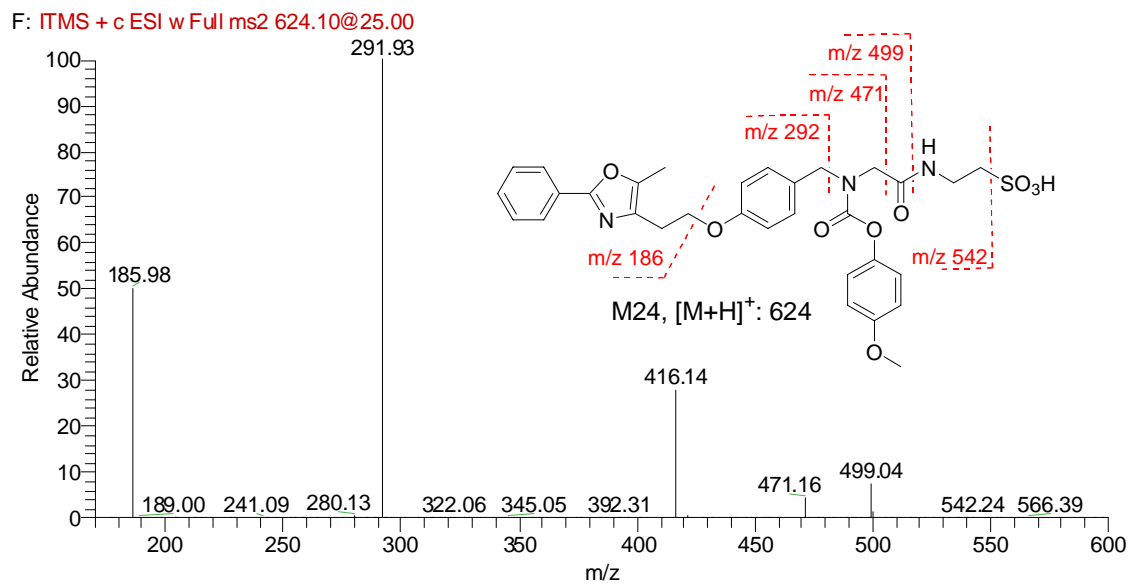
# Figure 2

# Figure 3

# Figure 4

# Figure 5

# Figure 6

F: ITMS + c ESI d w Full ms2 840.00@35.00

MS/MS of M30

308.13
[GSH+H]+ and
[m/z 840 -GSH-225]

m/z 711
m/z 765
m/z 615
m/z 597

m/z 693: 711- 18 (H₂O)
m/z 468 : 597-129

**M30**, [M+H]+: 840

265.13   346.96   411.66   468.14   589.53   597.24   615.06   693.08   711.10   765.18



F: ITMS + c ESI w Full ms3 840.00@35.00 308.00@35.00

MS/MS of m/z 308 ion

179.04

Fragment ions derived from [GSH+H]+: m/z 162, 179, 233
Fragment ions derived from [m/z 840 -GSH-225]: m/z 187, 265

146.12   161.93   187.05   215.13   233.06   265.09

# Figure 7



**M29a**, [M+H]$^+$: 856

MS/MS of M29a
m/z 820:  856-18-18
m/z 745:  856-18-18-75
m/z 709:  856-18-129
m/z 691:  856-18-18-129
m/z 595:  856-18-18-225
m/z 515 : 856-18-18-305
m/z 290:  856-18-18-225-305

F: ITMS + c ESI w Full ms2 856.00@35.00

# Figure 8



MS/MS of M29b
m/z 820: 856-18-18
m/z 763: 856-18-75
m/z 709: 856-18-129
m/z 691: 856-18-18-129
m/z 613: 856-18-225
m/z 533: 856-18-305
m/z 484: 856-18-225-129
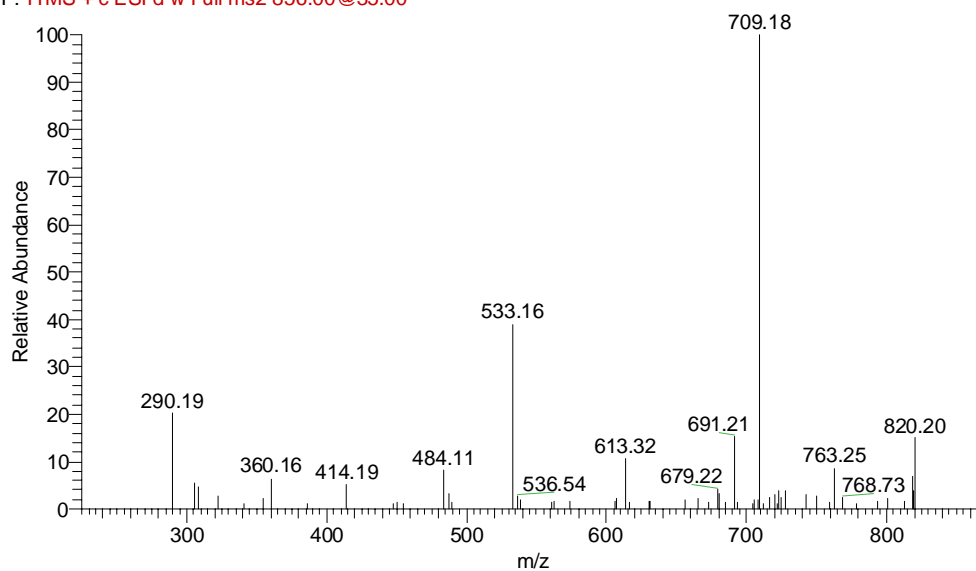m/z 290: 856-18-18-225-305

**M29b**, [M+H]$^+$: 856

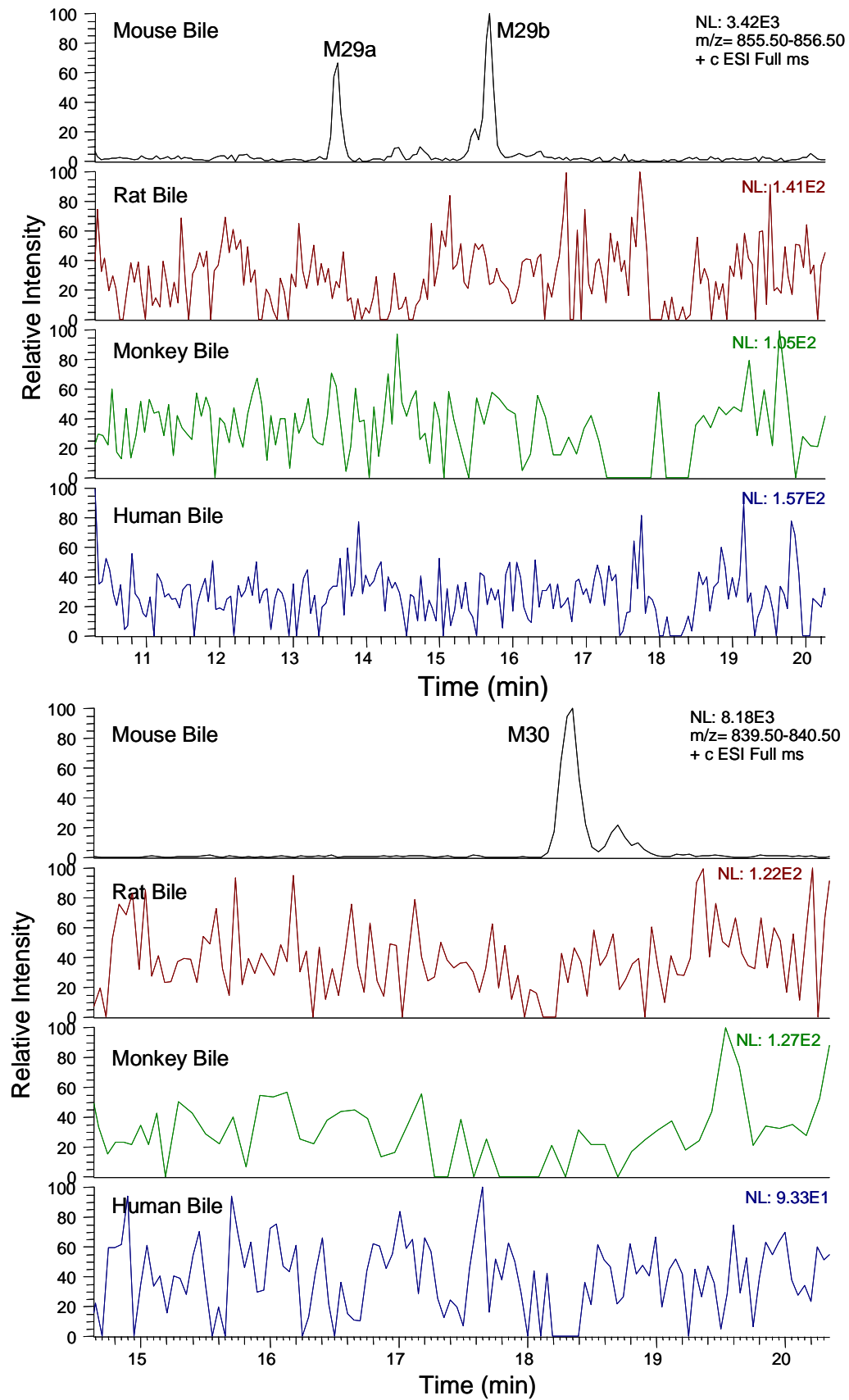F: ITMS + c ESI d w Full ms2 856.00@35.00

# Figure 9

# Figure 10

# Figure 11